PHYSICOCHEMICAL PROBLEMS
OF MATERIALS PROTECTION

Corrosion Inhibition of st37 Steel in Geothermal Fluid by *Quercus robur* and Pomegranate Peels Extracts

A. Buyuksagis[a],*, M. Dilek[b] and M. Kargioglu[a]

[a]*Afyon Kocatepe University, Science and Literature Faculty, Afyon, Turkey*
[b]*Afyon Kocatepe University, Engineering Faculty, Afyon, Turkey*
e-mail: absagis@aku.edu.tr
Received March 03, 2014

Abstract—Plant extracts have become important as an environmentally acceptable, readily available and renewable source of wide range of inhibitors. Tannins, a class of natural, non-toxic and biodegradable polyphenolic compounds, extracted from plant sources are already used as corrosion inhibitors in aqueous media. This study investigates the inhibiting effect of *Quercus robur* and pomegranate peels extracts on st37 steel corrosion in geothermal fluid using the Tafel polarization method. It was found that the extracts act as good corrosion inhibitors for geothermal fluid. 250 ppm of *Quercus robur* oak extract was seen to have 90% corrosion inhibition efficiency. The values of pH, potential, conductivity, total hardness and Ca^{2+} hardness, dissolved solid substance (TDS) and salinity of geothermal fluid were analyzed before and after the addition of extract into it. According to these analyses, increasing pH level more than 5 indicates that corrosion constructive aggressive ions (H^+) decrease. Furthermore the decrease of conductivity values as a result of the decrease of inhibitor concentration shows that corrosion slows down. Ryznar and Langelier Indexes are calculated for AF11 well, reinjection and collected pools. The values of indexes show that geothermal fluid is corrosive and scale properties.

INTRODUCTION

Formation of scale is one of the important events that occur during the utilization of geothermal fluid and affect the lifetime of system and productivity. The main reason of scale formation, which becomes related to degassing, evaporating and cooling, is the relative dissolubility of $CaCO_3$. It is important to know the scale formation of mechanism and to understand it well in the process of choosing measures and cleaning method of mechanism [1–7]. The corrosion effect of geothermal fluid is related to chemical composition of medium very much. Besides ions which make corrosion, pH changes, which depend on the loosing of CO_2 in medium, are the other parameters that affect the corrosion. The use of inhibitors is one of the most practical methods for protection against corrosion. Among numerous inhibitors that have been tested and applied industrially as corrosion inhibitors, those that are non-toxic or low toxic are now far more strategic than in the recent past. In the 21st century, the research in the field of "green" or "eco-friendly" corrosion inhibitors has been addressed toward the goal of using cheap, effective compounds at low or "zero" environmental impact. Plant extract is low cost and environmentally safe, and so the main advantage of using plant extract as the corrosion inhibitor is due to both economic and environmental benefits [8, 9]. The basic nature of plant extract inhibitors will be effectively inhibiting the corrosion of metals under various environments and especially in acid medium [10].

Tannins are the class of polyphenolic compounds which are natural, non-toxic and can be biodegradable with bacteria. The tannins extracted from plant sources are used as corrosion inhibitor in dilute solutions, as rust transformer compounds, as pigment in dyes, as corrosion inhibitor for steels in concrete, oxygen keeper in the system of iron-based deposits and boiler water treatment. Tannins are divided into two polymeric classes as the tannins which can be hydrolyzed and the tannins which are condensed. Hydrolyzed tannins are the gallic or egallic acids which can be hydrolyzed in acidic medium. The condensed tannins are the polymeric flavanoids. The hydrolysable tannin is usually found in chestnut tree [11].

The condensed tannin is obtained from the wattle tree like mimosa tannin. Oak tannin (condensed tannin) is used very long time in the inhibition studies.

Up to now, many plant extracts have been used as effective corrosion inhibitors of iron or steel in various media, such as tannins are applied both in solvents and in waterborne pretreatment systems. Although there are many studies on the metallic corrosion inhibition and the protection of different tannin extract, there is little information about the corrosion activity of *Quercus robur* oak and pomegranate peels. *Quercus robur* oak is a nut in Turkey which is long-shaped, hard and

---

[1] The article is published in the original.

smooth, placed in a cup, rich in tannin and seems like hazel-nut. Pomegranates include tannins, too. They include especially hydrolysable tannins. One of the most known is punicalagings aqueous extract of *Zallouh root* [12,13], extracts of leaves of *Nypa fruticans Wurmb* [14], *Khillah* extract [15]. *Mangrove* tannins and their flavanoid monomers [16], *Occimum viridis* extract [7], *Sansevieria trifasciata* extract are studied as inhibitor [17]. Various plant extracts, aqueous extract of *olive leaves* [18], aqueous extract of *Zallouh* root [19] and *Eugenol* derivatives [20]. *Pennyroyal* oil from *Mentha pulegium* are examined in HCl solutions with regard to the inhibition effects on the corrosion of steel [21]. Inhibition extract has increased as the concentration increases. *Zenthoxylum alatum plant* is examined in ortophosphoric acidic solutions with regard to the inhibition effects on the corrosion of soft steel [19]. It shows 88% inhibition at 70°C. The extracts of *May Chamomile* [21], *Chamomile* (*Chamaemelum mixtum* L.), *Halfabar* (*Cymbopogon proximus*), *Black cumin* (*Nigella sativa* L.) and *Kidney bean* (*Phaselous vulgaris* L.) plants are examined in 1 M sulphuric acidic medium with regard to the inhibition effects on the corrosion of steel by using electrochemical impedance spectroscopy and potantiodynamic polarization techniques. The experimental results show that Black cumin, Kidney bean, *Chamomile* and *Halfabar* plants can be used as perfect inhibitor for steel in the medium with sulphuric acid. It is observed that as the plant extracts concentration increases, the effect of inhibition increases and it is determined that it is related to the formation of stable plant extract complex on the steel surface of inhibition mechanism. Furthermore, it is found that the inhibition effects of these plant extracts have increased relatively as follows: *Black cumin > Kidney bean > Chamomile > Halfabar.*

The aim of this study is to determine the reasons of corrosion and scale formation events in the city of Afyonkarahisar's heating network, where used geothermal fluid as heating source, by water analyses and electrochemical method. In this study, the corrosion preventing character of the tannin which is extracted from *Quercus robur* oak and pomegranates peel extracts are examined. Extract concentrations are chosen as 250, 500, 1000, 2000 and 3000 mgL^{-1}. It is found that the extracts have shown the inhibition in the geothermal fluid as a result of the experimental studies.

EXPERIMENTAL

Obtaining of Extract

The *Quercus robur* oaks which are the nuts of oak trees are collected in Afyonkarahisar's central Hidirlik place. Pomegranates are bought from bazaar. The nuts of the *Quercus robur* oaks are blended after they are peeled and they are divided into small pieces. The same process is repeated for the pomegranates peels. The samples are dried for 5 days under the room temperature. The dried samples are kept in water bath with

methanol adjusted 40°C for 3 days [20−22]. After that the parts of *Quercus robur* oaks and pomegranates peels are separated from their extracts with methanol by filtering process. Methanol is removed from the mixture by using rotary evaporator under the vacuum [23−26]. A viscose liquid with dark brown color is obtained. The viscose liquid is dissolved a little in HCl in order to prepare stock solutions and then double distilled water is added into it and after that ethyl alcohol, in the amount of 25%, is added into it in order not to cause degradation of stock solution. The other concentrations are prepared from this solution.

Geothermal Fluid Analyses

The geothermal fluid is taken from AF 11 well, which is one of AFJET wells, in order to examine corrosion and scale formation. All experiments have been carried out in this AF 11 well geothermal fluid. The tannin extracts are used corrosion inhibitors. The tannin extracts (as 250, 500, 1000, 2000 and 3000 mgL^{-1} concentrations) are added into AF 11 well geothermal fluid. pH and potential values of the geothermal fluid (with and without inhibitors) are measured by WTW pH 330i/SET pH meter and the conductivity and total dissolved solid substance (TDS) are measured by WTW cond 330i/SET conduct meter. Total hardness experiments are carried out according to Turkish Standart and previous works [27−29]. Ryznar and Langelier Index calculations are calculated as it is given in 27−29 articles [28−30]. In this study, ion chromatography (IC-Dionex; GP50) and inductively coupled plasma optical emission spectroscopy (ICP-OES; ICP-AES Varian Liberty Series2 EL97093438) analyses were carried out on the geothermal fluid samples (AF11, collected pool, reinjection) that are taken off Afyonkarahisar Geothermal Heating System.

Electrochemical Measurements

The electrochemical measurements were made by using a three-electrode cell assembly at room temperature. The working electrode was a st37 steel, has 0.19625 cm^2 exposed surface area and the rest being covered by using commercially available teflon and following chemical composition [wt]; C (0.10%), Mn (0.40%), Si (0.25%), P (0.45%), S (0.45%) and Fe (remainder). A platinum foil was used as counter electrode and saturated calomel electrode (SCE) as reference electrode. All potentials obtained from experiments are measured against SCE and the results are given according to this electrode. SCE is brought near to working electrode by the help of Lugin-Haber capillary in order to prevent potential decrease between the SCE and the working electrode. The working electrodes are polished with sand paper in 1200 grid before starting the experiment and it is washed with bidistilled water. And then it is dipped into the geothermal fuid. The magnetic bar is used in order to work in a more

Table 1. The corrosion characteristics of st 37 steel in AF11 and AF11 + x mgL^{-1} pomegranates peels and *Quercus robur* oak extracts concentrations at 25°C.

		$-E_{cor}$ (mV)	$-\beta_c$ (mV)	β_a (mV)	i_{cor} μAcm^{-2}	% inh. (η)	Surface coated fraction (θ)
	AF11	540	222	200	10.00	–	–
Pomegranate peel extract	3000 mgL^{-1}	660	526	606	6.30	37.0	0.37
	2000 mgL^{-1}	675	454	588	3.16	68.0	0.68
	1000 mgL^{-1}	570	250	333	1.58	84.0	0.84
	500 mgL^{-1}	670	200	100	1.00	90.0	0.90
	250 mgL^{-1}	530	100	100	1.58	84.0	0.84
Quercus robur extract	3000 mgL^{-1}	610	200	200	4.00	60.0	0.60
	2000 mgL^{-1}	560	200	167	3.16	68.0	0.68
	1000 mgL^{-1}	560	167	250	2.60	74.0	0.74
	500 mgL^{-1}	550	143	111	1.58	84.0	0.84
	250 mgL^{-1}	490	83	71.4	1.00	90.0	0.90

homogenous medium by removing the occurred corrosion productions from the metal surface. The current-potential curves are obtained in the scanning rate in 2 mVs^{-1} by potentiodynamic method. Prior to the electrochemical measurement, a stabilization period of 30 min. was allowed, which was proved to be sufficient to attain a stable value of E_{corr} of st37 steel in geothermal fluid [6, 31] Pentium IV computer is used because it is performed in Wenking PGS 2000D model potantiostat/galvanostat, the working computer-based program. The corrosion characteristics as corrosion rate (i_{cor}), corrosion potential (E_{cor}), anodic and cathodic Tafel slopes (β_a and β_c) surface coating fraction (θ) and percentage inhibition efficiency (IE%) values are determined in this study.

Surface Analyses

SEM analyses from the st37 steel surface have been obtained by LEO 1430 VP scanning electron microscope. EDS spectrums are also taken over same samples. Before that SEM analysis the surface of st 37 steel have been prepared by using metallographic methods. Each alloy firstly have been ground from rough emery paper to fine emery paper (120–1200 grit paper) by using Metkon Gripo 2V Grinder Polisher (250–300 tour or period/min). Then st 37 steel is washed using bidistilled water. And then st 37 steel have been washed with alcohol and dried warm air current. St37 steel is waited in the geothermal fluid taken from AF 11 well for 2 and 9 days without inhibitor and it is waited in the 250 mgL^{-1} *Quercus robur* oak extract for 2 and 9 days. Microphotographs were taken from the st37 surfaces.

RESULTS AND DISCUSSION

The Results of Corrosion Experiments

The geothermal fluid is taken from AF 11 well which is one of the wells of Omer-Gecek area of Afyon City Geothermal Heating System (AFJET). In this study, the extracts of pomegranates peel and *Quercus robur* oak are used as corrosion inhibitor in order to prevent corrosion and scale formation occurred in the geothermal heating system. The corrosion characteristics and the values of inhibitor efficiency at different extract concentrations are listed in Table 1. The reproducibility of results obtained for the percentage inhibition efficiency values for triplicate specimens were precise too. This indicates good reproducibility. Table 1 indicates that all extracts act as good corrosion inhibitor for the corrosion of st 37 steel in geothermal fluid.

When Table 1 is examined, % inhibition increases as the inhibitor concentration decreases. According to Yan et al. (2008) [32] and Singh et al. (2012) [33] an inhibitor can be classified as cathodic or anodic type if the displacement in corrosion potential is more than 85 mV/SCE, with respect to corrosion potential of the blank [32, 33]. Presence of pomegranate peel, the corrosion potential (E_{corr}) of st 37 steel is shifted to the range (10−135 mV) mV/SCE, compared to the blank. This confirms that pomegranate peel extract acts as mixed-type inhibitor [34−38] The active rust compounds have been converted into more stable and resistant against corrosion in the presence of extract. It is found that there is a fast reaction between rust iron and natural tannin. The conversion of rust iron into blue-black coating can be explained that iron oxide and oxyhydroxides form complex with the polyphenolic part of tannin (The conversion of rust iron into blue-black coating can be explained by formation of complex with the polyphenolic part of tannin by iron
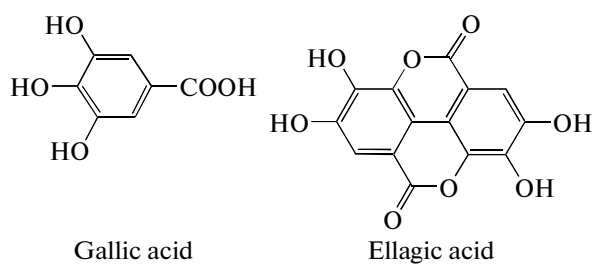
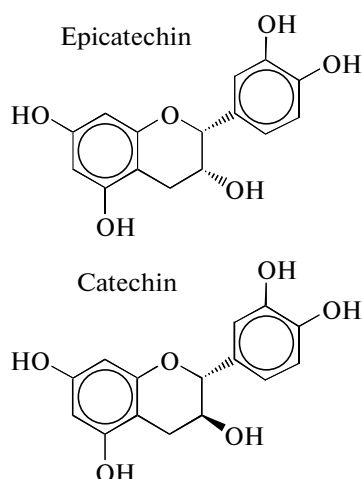Fig. 1. The hydrolysable tannins.

Fig. 2. The condensed tannins.

Fig. 3. Tafel curves for st37 steel in AF 11 well and AF 11+ x mgL^{-1} *Quercus robur* oak extract.
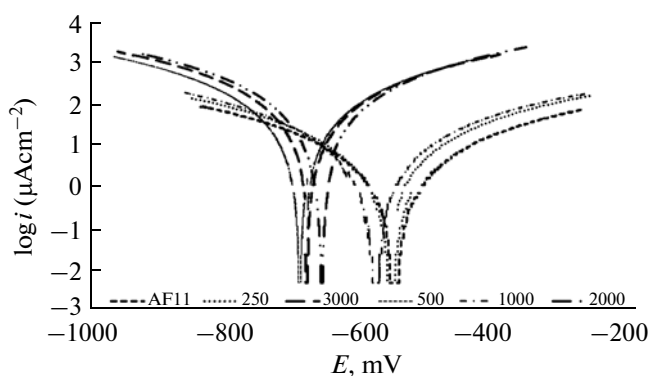
Fig. 4. Tafel curves for st37 steel in AF 11 well and AF 11+ x mgL^{-1} pomegranates peels extract.

oxide and oxyhydroxides). Tafel curves for st37 steel in geothermal fluid containing different concentrations of plant extract are shown in Figs. 3 and 4 [11].

Further inspection of Figs. 3 and 4 reveals linear relationship; inspection of Table 1 reveals that the IE% increases as the concentration of the extract is decreased. Moreover, the Tafel slopes do not suffer significant variation with decrease of *Quercus robur* (Fig. 3) concentration suggesting that the presence of inhibitor in the test solution does not modify the process mechanism and act as adsorptive inhibitor, retarding both cathodic and anodic reaction by blocking the active sites [39–41]. The polarization measurements indicated that the extract inhibits the corrosion processes by blocking the available active cathodic and anodic sites of the metal surface through adsorption of the chemical constituents of the extract on the metal/solution interface. This phenomenon could take place via dipole-type interaction between unshared electron pairs of oxygen atom or p electrons-interaction with the vacant, low energy d-orbitals of Fe surface atoms (anodic sites) [40, 42, 43].

In the presence of *Quercus robur*, the corrosion potential (E_{corr}) of st 37 steel was shifted to the range (10–70) mV/SCE, compared to the blank. T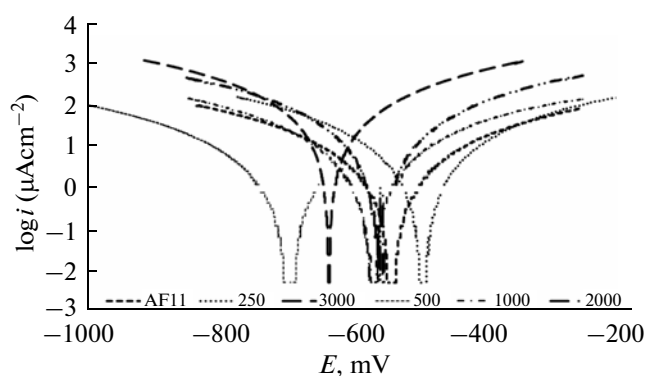his confirms that *Quercus robur* extract acts as mixed-type inhibitor [42–44]. The observed decrease of the current densities (i_{corr}) with the decrease in *Quercus robur* extracts concentration, indicates the increased inhibition efficiency with the decrease in the concentration of the inhibitor. This reflects also, the formation of anodic protective films containing oxides and *Quercus robur* oak extract [45].

The results clearly showed that the inhibition mechanism involves blocking of steel surface by inhibitor molecules via adsorption [46–48]. In general, the phenomenon of adsorption is influenced by the nature of metal and chemical structure of inhibitor. The values of thermodynamic parameters for the adsorption of inhibitors can provide valuable information about the mechanism of corrosion inhibition [35, 49].

Results of the present investigation (Table 1) involving extracts of *Quercus robur* and pomegranate peel indicate that the inhibition efficiency increases with decrease in extracts' concentration and the maximum inhibition efficiency was obtained with 250 mgL^{-1} concentration within the range of concentrations studied. Corrosion inhibition is initiated by the displacement of adsorbed water molecules by the inhibitor species leading to specific adsorption on the metal surface

[46, 50]. It has also been reported that the adsorption of the heterocyclic compounds occurs with the aromatic rings sometimes parallel but mostly normal to the iron surface [51]. The solubility of the formed iron complex depends on the molecules of inhibitor and hydroxyl groups and also determines degree of corrosion inhibition.

Plant extracts inhibit the dissolution reaction by adsorption at the metal surface in two different ways: physical adsorption (physisorption) and/or chemical adsorption (chemisorption) [10, 52, 53]. The adsorbed layer acts as a barrier between the metal surface and the corrosive environment, causing reduction in the corrosion rate [54]. This makes this inhibitor, in addition to its environmentally friendliness and abundant availability, a viable corrosion inhibitor in a wide range of oil and gas environments where acid gases such as CO_2 and H_2S in the presence of water are the major corrodents. With the addition of pomegranate peel and *Quercus robur* extracts, inhibitor molecules are adsorbed on the st 37 steel surface and interaction between them can be described by adsorption isotherms. The most widely used adsorption isotherms are the Bockris-Swinkel, Flory Huggins, Frumkin, Temkin, El-Awady and Langmuir isotherm [45, 47, 55−57]. The inhibition efficiency (IE%) is directly proportional to the fraction of the surface covered by the adsorbed inhibitor. The corrosion-inhibiting effect of S. mombin L. extract can be attributed to phytochemical constituents including alkaloids tannins, saponins, flavonoids, ascorbic acid, riboflavin thiamine and nicotinic acid. The different constituents may react with freshly generated Fe^{2+} ions on a corroding metal surface forming organometallic [Fe-Inh] complexes. The inhibiting effect of such complexes then depends on their stability and solubility in the aqueous corrodent [58]. As can be seen by the good fit at Fig. 5, these plant extracts as inhibitor found to obey Temkin adsorption isotherm [59, 60]. The simplest, being the Temkin isotherm, is based on assumption that all adsorption sites are equivalent and that Temkin adsorption equation is [61]

$$\theta = a + b\log c.$$

Geothermal Fluid Analyses

The potential, salinity, conductivity, total dissolved substances (TDS), total hardness and pH values were measured in AF 11 well and AF11 well + x mgL^{-1} pomegranates peels and *Quercus robur* oak extracts' concentrations are listed in Table 2.

The analysis of pH given in Table 2 shows that, as the extract concentration decreases, pH value increases and % inhibition values increase, too. The increase of pH is effective on the decrease of corrosion. pH values of 250 mgL^{-1} pomegranates peel and 250 mgL^{-1} *Quercus robur* oak extracts are 6.73 and 7.70 respectively close to neutral. In neutral mediums,
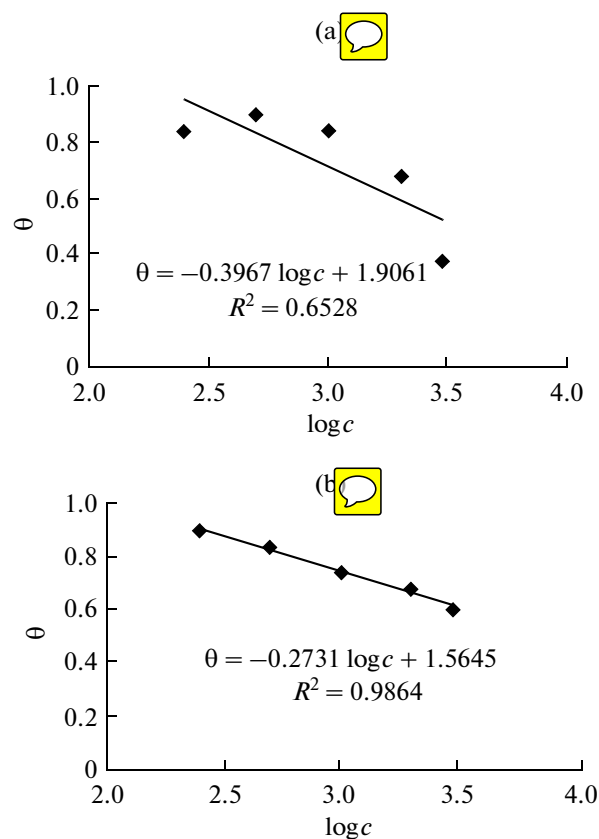

Fig. 5. Temkin adsorption isotherm.

general corrosion rate decreases because of the decrease of active surface, which is faced commonly and rather effective on the passivity state. As pH of the fluid increases, the reaction of scale formation decreases. The corrosion rate increases when pH is below 8, the inhibition decreases. As water is acidic, it increases the corrosion and as a result of the dissolution of the occurred scale, the contact between the metal and the geothermal fluid increases. The corrosion is more effective in acidic water. Because the surface of the metal is bare and it is not coated with hydroxides and oxides. As the conductivity increases because of salts (dissolved oxygen, H^+ ion, Cl^- ion, H_2S, CO_2, NH_3, SO_4^{2-}, HCO_3^- and CO_3^{2-} ion) occurred in the geothermal, the corrosion increases, too. On the other hand, the inhibition decreases. The increase of TDS gets the corrosion increased. The increasing TDS gets the conductivity and salinity increased, which gets the corrosion increased. The surface coating fraction is approximately 0.37 and 0.90 (Table 1). The adsorbed substance's surface coating fraction may be approximately $\theta \longrightarrow 1$. In other words, the rates of the probable reactions slow down on the surface, because almost all the parts of the surface are coated. Ca^{2+} and Mg^{2+} form hardness in waters. The hardness alone does not create any problem. A calcium solution leads to hardness in pH 3, too. However, it forms no

Table 2. The potential, salinity, conductivity, TDS, total hardness and permanent hardness values measured in AF 11 well and AF11 well + $x$mgL^{-1} pomegranates peels and *Quercus robur* oak concentrations extracts

		$-U$ (mV)	Salinity	Conductivity mS cm^{-1} $k = 0104$ (cm^{-1})	TDS (mg L^{-1}) 0.45	Total hardness (FSD)	Permanent hardness (FSD)	pH
	AF11	58.9	0.7	1.62	820	44	40.84	8.08
Pomegranate peel extract	3000 mgL^{-1}	282.4	2.1	3.57	1844	26	26.00	1.66
	2000 mgL^{-1}	273.7	0.9	1.88	908	39	39.00	1.92
	1000 mgL^{-1}	89.0	0.4	1.22	624	48	47.70	5.12
	500 mgL^{-1}	7.5	0.3	0.90	470	45	43.76	6.48
	250 mgL^{-1}	8.6	0.4	1.21	632	45	43.40	6.73
Quercus robur oak extract	3000 mgL^{-1}	307.7	4.9	7.66	2192	110	110.00	1.33
	2000 mgL^{-1}	301.4	1.6	2.84	1461	30	30.00	1.56
	1000 mgL^{-1}	73.2	0.0	0.47	212	44	37.20	7.90
	500 mgL^{-1}	60.2	0.0	0.26	116	10	8.00	7.60
	250 mgL^{-1}	66.5	0.0	0.13	59	10	9.00	7.70

Table 3. TDS, Ca hardness, alkaline hardness and total hardness, pH measuring values and the calculated pHs values of AF11 well, collection pool and reinjection

Sample	TDS (mgL^{-1})	Ca^{2+} hardness (mgL^{-1})	Alkaline hardness (mgL^{-1})	Total hardness (FSD)	pH	pH$_s$
AF11	801	144	192	44.40	7.80	7.61
Collected pool	801	144	192	43.75	7.52	7.61
Reinjection	802	143	194	45.00	7.60	7.60

deposit. The presence of Ca^{2+}, Mg^{2+} and alkalinity combination may lead to hardness and scale formation in the water [33]. The scale formation on the surfaces of heat transfer gets the heat transfer decreased. If the scale is inside of the pipe, it limits the flow of the fluid. The formation rate of $CaCO_3$ and $Mg(OH)_2$ is related to temperature, pH, the concentration of bicorbonate ions, the release rate of CO_2, the concentration of Ca^{2+} and Mg^{2+} ions and the amount of total dissolved substance (TDS) [29, 30, 62–64].

Furthermore, calcium hardness, alkaline hardness, saturated pH (pHs) and the calculated Langelier Saturated Index and Ryznar Stability Index values in AF11 well, collection pool and reinjection are shown in Table 3.

Geothermal fluids coming from all the wells are generally collected in the collection pool in AFJET geothermal heating system and inhibitor is added into it. After the gasses (O_2, CO_2, H_2S, NH_3 etc.) occurred in the dissolved form inside of it are removed, geothermal fluid is carried. Geothermal fluid used for heating in the city comes back again and it is pumped into the heating system by reinjection. TDS is the general indicator of the quality of water spring. As TDS increases, the quality of water goes bad.

When LSI values are −0.09 and 0.19 reinjection and AF11 well respectively, index values (Table 4) show that geothermal fluid is little corrosive and there has been no scale. LSI value of AF11 well is +0.19. This value shows that geothermal fluid is in equilibrium; however, there can be pitting corrosion. It can be seen that TDS values (Table 3) are not effective on the calculation of LSI values. According to these values LSI values show that the system is in equilibrium, however, there can be pitting corrosion.

RSI values (Table 4) has been changing between the values 7.42 and 7.70 pH = 7.80 is in AF11 well fluid and alkalinite hardness is 192, which shows that there is serious corrosion in AF11 well.

If pH value is little more than saturated pHs value, LSI is negative and water is in the very limited sediment potential. If the real pH is more than pHs, LSI is positive and water is saturated with $CaCO_3$ and it shows tendency to scale. The increasing positive LSI values get increased the potential of the scale formation. LSI only shows the driving power of water. Ca's higher concentration, TDS and alkalinity increase the tendency of the formation of scale. When RSI and LSI values (Table 4) are compared with the system, there has been corrosion

Table 4. The calculated LSI and RSI values and interpretation of AF11 well collection pool and reinjection

Sample	LSI index	RSI index	Interpretation LSI	Interpretation RSI
AF11	0.19	7.42	In equilibrium but pitting corrosion is possible	Serious corrosion
Reinjection	−0.09	7.70	Light corrosive but no scale formation	Heavy corrosion formation
Collectedpool	0.00	7.60	In equilibrium but pitting corrosion is possible	Heavy corrosion formation

Table 5. ICP-OES analysis results of AF11 well. collection pool and reinjection (as mg L^{-1})

Sample	Al	B	Ba	Ca	Cu	Cr	Fe	K	Li	Mg	Na	Zn
AF11	0.223	5.856	0.119	69.670	0.043	0.008	0.254	125.554	5.071	13.229	9.695	0.068
Collection pool	0.214	5.926	0.119	69.639	0.036	0.010	0.167	125.811	5.066	13.367	8.711	0.069
Reinjection	0.291	6.153	0.110	69.594	0.041	0.009	0.151	131.128	5.302	13.406	5.038	0.102

Table 6. The calculated from EDX analysis Na^+/Ca^{2+} ratios

Sample	Na^+/Ca^{2+} ratios
st 37 steel waited AF11 for 2 days	2.26
st 37 steel waited AF11 + 250 mgL^{-1} Quercus robur inhibitor for 2 days	1.68
st 37 steel waited AF11 for 9 days	5.24
st 37 steel waited AF11 + 250 mgL^{-1} Quercus robur inhibitor for 9 days	8.29

in both values. RSI shows that there has been a serious corrosion in all system generally.

RSI and LSI values (Table 4) give information about the formation of corrosion and scale. It gives important information about the rightness of scale formation. pHs values are to be average 7.60. There has been light scale formation only in AF11 well. If pHs value is close to $CaCO_3$'s saturated value, it is on the limit of scale formation. The fluid used in the system has corrosive character. There has been little scale formation. As it is seen, there is a tendency to corrosion in AFJET and there is no scale formation. It is resulted from the using of preventing commercial inhibitor of scale formation.

The Results of ICP-OES Analyses

The geothermal fluid used in AFJET geothermal heating system should be evaluated with its corrosive character instead of its scale formation character. ICP-OES analyses of the geothermal fluid samples taken from AF 11well, reinjection and collection pool are given in Table 5.

The temperature of the fluid taken from AF 11 well is 110°C. This shows that the geothermal fluid of this well is located in the average geothermal group. All fluid samples include Ca^{2+} ions highly, which supports $CaCO_3$ formation. Ca^{2+} concentration in geothermal fluid is related to dissolubility of $CaCO_3$ (calcite, aragonite), $CaSO_4$ (anhydride, jips), CaF_2 (florid) and other calcium minerals which are observed in the nature commonly.

In the systems, which have high temperature, Ca^{2+} concentration dissolved in hot water is generally upper than 50 mgL^{-1}. Ca^{2+} content of AF11 well is 69.670 mgL^{-1}. It is 69.639 mgL^{-1} in collection pool. In reinjection, Ca^{2+} concentration decreases to 69.594 ppm. The reason of decreasing may be explained as that $CaCO_3$ precipitates depending on loosing CO_2. Na^+/Ca^{2+} ratios are used as geothermometer. These values are calculated from EDX results for st37 steel surface; and are given Table 6.

It is accepted that high values show the direct feed from reservoir [20, 63]. Mg^{2+} concentration in geothermal fluid which has high temperature is between 1×10^{-3} and 1×10^{-1} mgL^{-1}. The higher concentrations (Table 5) show the concentration coming from rock close to surface or shallow water.

The scale formation of iron sulphur creates a serious problem. Iron sulphur is cathodic compared to iron. This forms galvanic cells which create serious cavitation corrosion. The occurrence of every kinds of precipitation in the waters which include the gases like H_2S, O_2 or CO_2 increases the intensity of probable corrosion problem. In the study and examinations performed in the majority of geothermal energy sources, especially in the compounds of scales occurred in steel pipes, element trace in a great amount is come across and resulted from the corrosion of metallic parts in the system (Table 5). In the waters
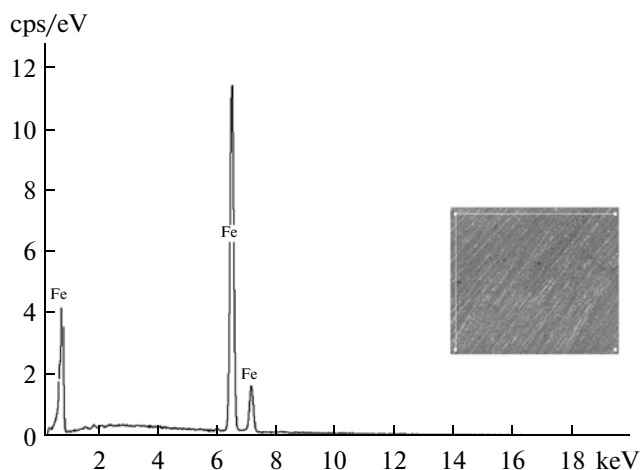
cps/eV

Fig. 6. The EDX analysis of bare st37 steel.
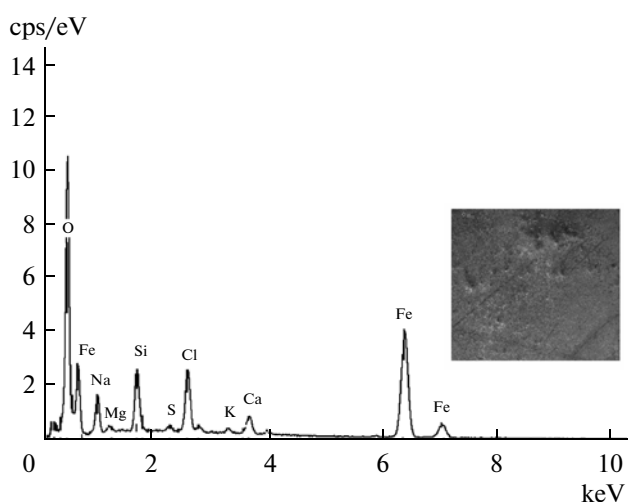
cps/eV

Fig. 7. The EDX analysis of st37 steel after waited in geothermal fluid AF11well for 2 days.
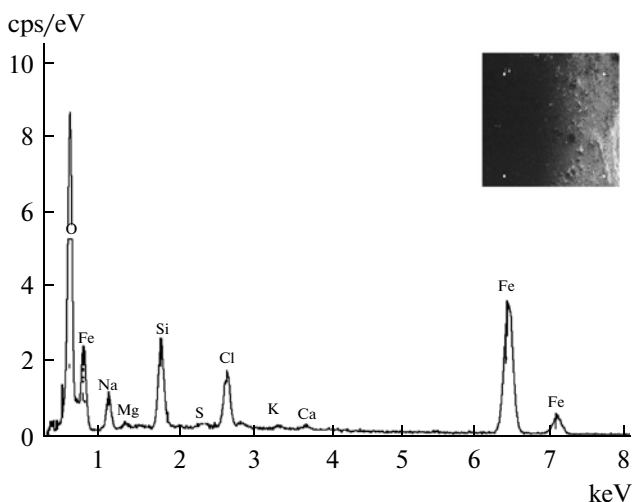
cps/eV

Fig. 8. The EDX analysis of st37 steel after waited in geothermal fluid AF11 for 9 days.

taken from geothermal pipe lines, P, Cr, Mn, Ni Mo trace elements resulted from steel corrosion are come across and in the minerals (like geotit, pyrite, opal), which are corrosion products, it is encountered with element traces resulted from steel corrosion by ICP-OES analysis (Table 5).

The resource and drilling waters belonging to Omer-Gecek Region show Na-Cl character for some samples and they show HCO_3^- character for some other samples. Furthermore, these waters include bor in increasing level [21, 63, 64].

The thermal fluid in Omer-Gecek geothermal region, where the temperatures are between 32 and 92°C, shows difference from the point of view. Omer-Gecek waters have usually the character of Na-Cl-HCO$_3$, which points out a probable deep water cycle. The mineral equilibrium is supervised by CO_2 concentration in a large scale [22]. Scale precipitation affects the metal corrosion. The protection is obtained against corrosion by precipitation of $CaCO_3$ scale sometimes intentionally. However, scale precipitation often accelerates corrosion.

The studied geothermal fluid samples (collection pool and reinjection) are the geothermal fluid samples, where inhibitor added, except for corrosion experiments (AF11 well). The fluid used in the system has more corrosive character. There is little scale formation. The reason of this, the commercial inhibitor used in AFJET shows the character that prevents scale formation. Geothermal fluid used in AFJET geothermal heating system should be evaluated with the corrosive character rather than scale formation.

The Results of Surface Analysis (SEM-EDX)

St 37 steel is waited in the geothermal fluid taken from AF 11 well in the solutions for 2 and 9 days without inhibitor and it is waited in the AF11+ 250 mgL^{-1} *Quercus robur* oak inhibitor for 2 and 9 days. Their EDX analyses are given in Figs. 6–10.

When the surface of st 37 steel, which is waited in geothermal fluid AF11 for 2 days (Fig. 7, Table 7), is examined, there are only Fe^{2+} and O^{2-} occurrences very much in the field analysis of surface. Fe^{3+} and O^{2-} form FeO_2^- anion. This is one of the corrosion products of iron. As a result of 100 μm EDX area scanning of st 37 steel waited in AF11 geothermal fluid for 2 days (Fig. 7), it is seen that the surface is homogenous and there are casting and sanding faults. The atoms found in the surface are O, Na, Mg, Si, S, Cl, K, Ca, Fe. It shows that this geothermal fluid dissolves many numbers of elements inside. The occurrences of Na$^+$ and Cl$^-$ on the surface show that geothermal fluid has the character of Na-Cl-HCO$_3$ [22]. The EDX analyses of st 37 steel after waited in geothermal fluid AF 11 and AF11+ 250 mgL^{-1} *Quercus robur* for 2 and 9 days with and without inhibitor are given Table 7.
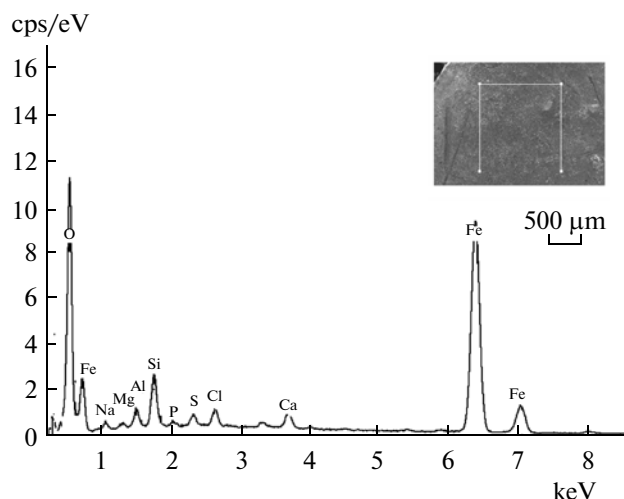
Fig. 9. The EDX analysis of st37 steel after waited in geothermal fluid AF11+250 mgL^{-1} *Quercus robur* oak extract for 2 days.
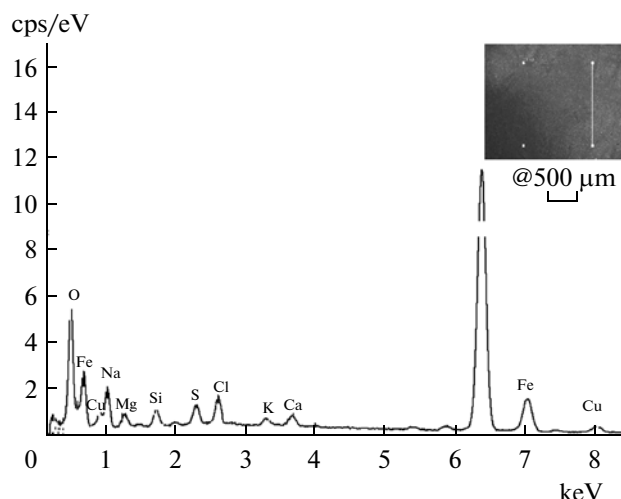
Fig. 10. The EDX analysis of st37 steel after waited in geothermal fluid AF11+ 250 mgL^{-1} *Quercus robur* oak extract for 9 days.

Literature shows that the corrosion inhibition is due to the formation of inhibitor film on the metal surface by inhibitor compounds. Analysis of geothermal fluid (with and without inhibitor) by EDX showed the presence of Fe−inhibitor complex along with iron oxides such as γ-Fe$_2$O$_3$ and γ-FeOOH. During mild steel dissolution reaction, FeOH and [FeClOH]$^-$ are formed as intermediates. These intermediates are converted to γ-Fe$_2$O$_3$ and γ-FeOOH and form oxide layer [65−67]. The intensity of oxygen molecules is higher than the carbon (Table 7) atom indicating presence of higher amount of iron oxides in the inhibitor film. On the other hand, with the presence of strongly adsorbable anion like Cl$^-$, the surface charge is changed to negative by specific adsorption of the anion, resulting in the joint adsorption of the anion with the cation [42]. The detection of chloride ions (Table 7) confirms the inclusion of chloride in the Fe-inhibitor complex. From the above evidences, the mechanism of film formation is as follows [58].

1. Formation of FeOH$^+$ and [FeClOH]$^-$ intermediates.

2. Conversion of FeOH$^+$ and [FeClOH]$^-$ to γ-Fe$_2$O$_3$ and γ-FeOOH and forms oxide layer.

3. At the pores of oxide layer, inhibitor molecules react with [FeClOH]$^-$ and forms more stable inhibitor complex and protects metal.

The corrosion products of Fe^{2+} are known as Fe(OH)$_2$, Fe(OH)$_3$, Fe$_3$O$_4$, Fe$_2$O$_3$ and FeO. The occurrences of Ca^{2+}, Mg^{2+} and Si^{2+} on the surface support the scale formation. When the scale comes into being on the surface, the part under the scale becomes anode. The other parts of it act as cathode and the material is holed by being exposing to pitting

Table 7. The EDX analyses of st37 steel after waited in geothermal fluid AF 11 and AF11+ 250 mgL^{-1} *Quercus robur oak extract* for 2 and 9 days

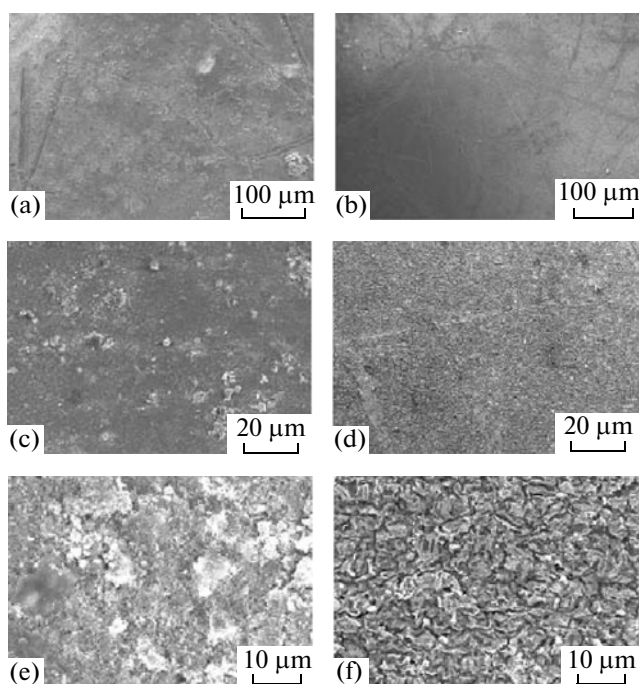|	C	O	Na	Mg	Al	Si	P	S	Cl	Ca	K	Cu	Fe
AF11 2 days	−	31.64	4.84	0.54	−	4.53	−	0.50	5.34	2.14	0.57	−	49.91
AF11+ *Quercus robur* 2 days	1.19	41.76	1.53	0.50	1.25	3.27	0.24	0.61	0.90	0.91	−	−	47.84
AF11 9 days	0.24	30.29	3.72	0.29	−	5.44	−	0.40	4.52	0.71	0.43	−	28.30
AF11+ *Quercus robur* 9 days	0.94	22.04	6.55	1.85	−	1.05	−	1.35	1.78	0.79	0.65	2.74	60.26

Not determined.
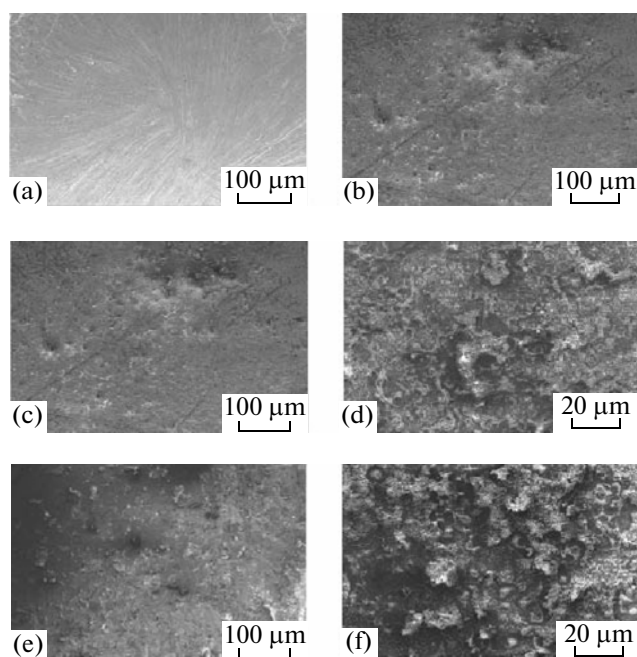
Fig. 11. The SEM microphotographs of st 37 steel with different magnificiations a—bare st37 steel b—AF11 + 2 days c—AF11 + 2 days d—AF11 + 2 days e—AF11 + 9 days f—AF11+ 9 days.

Fig. 12. The SEM microphotographs of st 37 steel in AF11+250 mgL^{-1} *Quercus robur* oak extract with different magnificiations a—AF11 + 2 days b—AF11 + 9 days c—AF 11 + 2 days d—AF11+ 9 days e—AF11 + 2 days f—AF 11 + 9 days.

corrosion. The excess Cl$^-$ supports the pitting corrosion. The oxygen existed on the surface supports the scale formation in the form of $CaCO_3$, $Mg(OH)_2$ and SiO_4.

St 37 steel is waited in the geothermal fluid taken from AF 11 well in the solutions for 2 and 9 days without inhibitor and it is waited in the 250 mgL^{-1} *Quercus robur* inhibitor solution for 2 and 9 days. Their SEM microphotographs are shown in Figs. 11−12.

When the surface of st 37 steel, which is waited in 250 mgL^{-1} *Quercus robur* AF11 for 2 days (Fig. 11b, 11c, 11d), is examined, it can be seen that the surface is very smooth and homogeneous and there are only sanding faults. The surface is homogenous and there are only sanding faults in the condition of st 37 steel before putting it into the solution. There becomes a protective film in the existence of inhibitor. When the surface of st 37 steel, which is waited in geothermal fluid AF11+ for 9 days (Fig. 11e, 11f), is examined, it can be seen that there is some roughness on the surface and there are much more rough structures and the contents of Na$^+$ and Cl$^-$ has been decreased compared with the values of 2 days waiting period (Table 7) of it and there are much more O^{2-} and Fe^{2+} on the surface. There have been existed iron hydroxides and oxides, which are corrosion products, on the surface. When the surface of st 37 steel (100 μm), which is waited in 250 ppm *Quercus robur* inhibitor solution geothermal fluid AF11+ for 9 days (Fig. 11e, 11f), is examined, it can be seen in element analyses that there are almost same values compared with 2 days waiting period of it.

The fact that the surface is not been destroyed shows that there occurs a film on the surface and it prevents the corrosion and scale formation. The field analyses carried out as a result of waiting of st 37 iron for 9 days in AF11, it can be seen that there occurs a complex in Fe_2O^{2+} structure on the surface. These are effective in the protection of the surface against corrosion and scale formation (Table 7).

When microphotographs of SEM are examined (Fig. 12), it can be seen that there are sanding faults in all photographs. When uncovered; st 37, AF11+ 2 days with inhibitor (Fig. 12a, 12c, 12e), AF11+ 9 days with inhibitor (Fig. 12b, 12d, 12f), it can be seen that surface images are similar to each other. The photographs with inhibitor (Fig. 12) are better than bare surface, which shows that inhibitors form a thin film on the surface and it makes the corrosion and scale formation decreased. The surfaces without inhibitor are rougher and they are not homogeneous (Fig. 11). The surfaces are exposed to corrosion. When EDXs of the samples above are examined (Table 7), there are usually FeO_2^- ions on the surface without inhibitor and there is Fe_2O^+ ion on the surface with inhibitor. Because there is excess of charge in FeO_2^-, it accelerates the corrosion. Fe_2O^+ makes the corrosion and scale formation decreased by holding on the surface. Iron hydroxides first and then transforms into oxides, while it is cor-

roded. Iron is corroded a little and corrosion products have produced a protective structure on the surface by uniting with inhibitors.

CONCLUSIONS

1. The geothermal fluid has corrosive character according to the calculated LSI and RSI values.

2. The scale formation is on the limit or occurs very little.

3. The increasing TDS, alkaline and hardness support scale formation.

4. 250 mgL^{-1} extracts of Quercus robur oak have showed 90 % inhibition efficiency. 500 mgL^{-1} extracts of pomegranate peel have showed 90 % inhibition efficiency.

5. The extracts are nature friendly and renewable inhibitors.

6. The extracts act as mixed inhibitors.

7. EDX analysis shows that there has been $CaCO_3$ scale formation in the system.

8. It is seen that the scale formation is on the limit or very little because there is inhibitor in the geothermal fluid samples taken for index calculations. The inhibitor used in the system prevents scale formation but it does not prevent corrosion. Both corrosion inhibitor and scale inhibitor should be added into the system in order to be able to prevent corrosion and scale formation.

9. It is seen that the form of geothermal fluid has Na-Cl-HCO_3 character in IC and ICP-OES analyses.

10. It is seen that Na/Ca ratio is feed from the reservoir.

11. The very high amount of Ca^{2+} supports $CaCO_3$ scale formation in ICP-OES analyses.

ACKNOWLEDGMENTS

REFERENCES

1. Banaś, J., Lelek-Borkowska, U., Mazurkiewicz, B., and Solarski, W., *Electrochim. Acta*, 2007, vol. 52, p. 5704.
2. Corsi, R., *Geothermics*, 1986, vol. 15, p. 839.
3. Richter, S., Hilbert, L.R., and Thorarinsdottir, R.I., *Corros. Sci.*, 2006, vol. 48, p. 1770.
4. Morizot, A.P. and Neville, A., *Colloid Interface Sci.*, 2002, vol. 245, p. 40.
5. Abiola, O.K., Otaigbe, J.O.E., and Kio, O.J., *Corros. Sci.*, 2009, vol. 51, p. 1879.
6. Abiola, O.K. and James, A.O., *Corros. Sci.*, 2010, vol. 52, p. 661.
7. Chauhan, L.R., *Corros. Sci.*, 2007, vol. 49, p. 1143.
8. Deng, S. and Li, X., *Corros. Sci.*, 2012, vol. 55, p. 407.
9. Raja, P.B., *Mater. Lett.*, 2008, vol. 62, p. 113.
10. Ibrahim, T., Alayan, H., and Mowaqet, Y., *Prog. Org. Coat.*, 2012, vol. 75, p. 456.
11. El-Etre, A.Y., *Mater. Chem. Phys.*, 2008, vol. 108, p. 278.
12. Orubite, K.O. and Oforka, N.C., *Mater. Lett.*, 2004, vol. 58, p. 1768.
13. El-Etre, A.Y., *App. Surf. Sci.*, 2006, vol. 252, p. 8521.
14. Rahim, A.A., Rocca, E., Steinmetz, J., et al., *Corros. Sci.*, 2007, vol. 49, p. 402.
15. Oguzie, E.E., *Mater. Chem. Phys.*, 2006, vol. 99, p. 441.
16. Oguzie, E.E., *Corros. Sci.*, 2007, vol. 49, p. 1527.
17. Gunasekaran, G. and Chauhan, L.R., *Electrochim. Acta*, 2004, vol. 49, p. 4387.
18. Abdel-Gaber, A.M., Abd-El-Nabey, B.A., Sidahmed, A., et al., *Corros. Sci.*, 2006, vol. 48, p. 2765.
19. Bouyanzer, A., Hammouti, B., and Majidi, B.L., *Mater. Lett.*, 2006, vol. 60, p. 2840.
20. Au, T.K., Lam, T.L., Ng, T.B., et al., *Life Sci.*, 2001, vol. 68, p. 1687.
21. Ilavarasan, R., Mallika, M., and Venkataraman, S., *J. Ethnopharmacol.*, 2006, vol. 103, p. 478.
22. Osadebe, P.O. and Okoye, F.B.C., *J. Ethnopharmacol.*, 2003, vol. 89, p. 19.
23. Chattopadhyay, D., Arunachalam, G., Mandal, A.B., et al., *J. Ethnopharmacol.*, 2003, vol. 85, p. 99.
24. Nwafor, P.A. and Bassey, A.I.L., *J. Ethnopharmacol.*, 2007, vol. 111, p. 619.
25. Troszynska, A., Amarowicz, R., Lamparski, G., et al., *Food Qual. Pref.*, 2006, vol. 17, p. 31.
26. Siddhuraju, P. and Manian, S., *Food Chem.*, 2007, vol. 105, p. 950.
27. *TS 266: Turkish standards, Drinking water standards.*
28. Buyuksagis, A. and Erol, S., *Thermal and Mineral Water Conf., April 24—25, 2008*, Afyonkarahisar, Turkey: Afyon Kocatepe Univ., 2008, p. 279.
29. Buyuksagis, A. and Erol, S., Thermal and Mineral Water Conf., April 24—25, 2008, *Afyonkarahisar, Turkey: Afyon Kocatepe Univ.*, 2008, p. 249.
30. Erol, S., *Master's Thesis*, Afyonkarahisar: Grad. School Nat. Appl. Sci., Afyonkarahisar Kocatepe Univ., 2008.
31. Quraishi, M.A., Singh, A., Singh, V.K., et al., *Mater. Chem. Phys.*, 2010, vol. 122, p. 114.
32. Yan, Y., Li, W., Cai, L., and Hou, B., *Electrochim. Acta*, 2008, vol. 53, p. 5953.
33. Singh, A., Ahamed, I., and Quraishi, M.A., *Arab. J. Chem.*, 2012, vol. 5.
34. Lecante, A., Robert, F., Blandini@res, P.A., and Roos, C., *Curr. Appl. Phys.*, 2011, vol. 11, p. 714.
35. Ostovari, A., Hoseinieh, S.M., Peikari, M., et al., *Corros. Sci.*, 2009, vol. 51, p. 1935.
36. da Rocha, J.C., da Cunha Ponciano Gomes, J.A., and D'Elia, E., *Corros. Sci.*, 2010, vol. 52, p. 2341.
37. Soltani, N., Tavakkoli, N., Khayatkashani, A., et al., *Corros. Sci.*, 2012, vol. 62, p. 122.
38. Al-Turkustani, A.M., Arab, S.T., and Al-Qarni, L.S.S., *J. Saudi Chem. Soc.*, 2011, vol. 15, p. 73.
39. Amin, M.A., Khaled, K.F. Mohsen, Q., and Arida, H.A., *Corros. Sci.*, 2010, vol. 52, p. 1684.

40. Bereket, G. and Yurt, A., *Corros. Sci.*, 2001, vol. 43, p. 1179.

41. Bobina, M., Kellenberger, A., Millet, J.P., et al., *Corros. Sci.*, 2013, vol. 69, p. 389.

42. Abdel-Gaber, A.M., Abd-El-Nabey, B.A., and Saadway, M., *Corros. Sci.*, 2009, vol. 51, p. 1038.

43. Lebrini, M., Robert, F., and Lecante, A., *Corros. Sci.*, 2011, vol. 53, p. 687.

44. El-Etre, A.Y., *Corros. Sci.*, 2003, vol. 45, p. 2485.

45. Hamdy, A. and El-Gendy Nour, Sh., *Egypt. J. Petrol.*, 2013, vol. 22, p. 17.

46. Eduok, U.M., Umoren, S.A., and Udoh, A.P., *Arab. J. Chem.*, 2013, vol. 5, p. 325.

47. Li, L., Zhang, X., Lei, J., et al., *Corros. Sci.*, 2012, vol. 63, p. 82.

48. de Souza, F.S. and Spinelli, A., *Corros. Sci.*, 2009, vol. 51, p. 642.

49. Bentiss, F., Lebrini, M., and Lagrené, M., *Corros. Sci.*, 2005, vol. 47, p. 2915.

50. Solmaz, R., Kardas, G., Yazici, B., and Erbil, M., *Colloids Surf., A*, 2008, vol. 312, p. 7.

51. Mikhaeil, B.R., Badria, F.A., Maatooq, G.T., et al., *J. Mater. Sci.,* 2009, vol. 44, p. 274.

53. Uwah, I.E., Okafor, P.C., and Ebiekpe, V.E., *Arab. J. Chem.,* 2013, vol. 6, p. 285.

54. Pandian, B.R. and Sethuraman, M.G., *Iran. J. Chem. Chem. Eng.*, 2009, vol. 28, p. 77.

55. Kumar, K.P.V., Pillai, M.S.N., and Thusnavis, G.R., *J. Mater Sci. Technol.*, 2011, vol. 27, p. 1143.

56. Obi-Egbedi, N.O., Obot, I.B., and Umoren, S.A., *Arab. J. Chem.*, 2012, vol. 5, p. 361.

57. Konojia, R. and Singh, G., *Surf. Eng.*, 2005, vol. 21, p. 180.

58. Satapathy, A.K., Gunasekaran, G., Sahoo, S.C., et al., *Corros. Sci.*, 2009, vol. 51, p. 2848.

59. Garai, S., Garai, S., Jaisankar, P., et al., *Corros. Sci.*, 2012, vol. 60, p. 193.

60. Raja, P.B. and Sethuraman, M.G., *Mater. Lett.*, 2008, vol. 62, p. 2977.

61. Gerengi, H., Schaefer, K., and Sahin, H.I., *J. Ind. Eng. Chem.*, 2012, vol. 18, p. 2204.

62. Mutlu, H., *PhD Thesis*, Ankara, 1996.

63. Akan, B. and Suer, S., *Thermal and Mineral Water Conf., April 24–25, 2008*, Afyonkarahisar, Turkey: Afyon Kocatepe Univ., 2008, p. 97.

64. Buyuksagis, A., *J. Geol. Eng. Assoc.*, 2008, vol. 31, p. 9.

65. Muralidharan, V.S. and Veerashanmugamani, M., *J. Appl. Electrochem.*, 1985, vol. 15, p. 675.

66. Macfarlane, D.R. and Smedley, S.I., *J. Electrochem. Soc.,* 1986, vol. 133, p. 2240.

67. Noor, E.A. and Al-Moubaraki, A.H., *Int. J. Electrochem. Sci.*, 2008, vol. 3, p. 806.

SPELL: 1. egallic, 2. flavanoids, 3. punicalagings